Supplementary Material I

March 19, 2019

Analysis of the Sherbrooke Test-Retest Data: Here, we empirically test how well our TN-PCA method and the HOOI method are able to model real structural connectomes. We use the Sherbrooke Test-Retest Dataset to determine whether the embeddings of networks from the two methods are reproducible. Recall that this dataset consists of three repeated scans of 11 subjects, yielding 33 total networks (for a particular feature, e.g., CSA feature); we stack these and subtract the mean to yield a $68 \times 68 \times 33$ tensor network. We apply our new semi-symmetric CP decomposition and the HOOI method to this data with different K, and investigate how well the low-dimensional embeddings, $\mathbf{U}_k$, are able to reproducible for the 11 subjects across scans, i.e., we perform a nearest neighbor classification using the embedding vector for each scan. Figure 1 shows the nearest neighbor classification result for each type of feature. Surprisingly, the HOOI method seems to do well for mid-range values of K, but the reproducibility of the low-dimensional embeddings gets worse for large K. This is likely due to the restrictiveness of the orthogonality constraint on $\mathbf{U}$ in the Tucker model which can lead to a poor model fit for tensor brain networks. Using this model to perform TN-PCA would require carefully tuning K to avoid lack-of-model fit issues. On the other hand, our new semi-symmetric CP model does not suffer from this problem; the performance tends to increase with

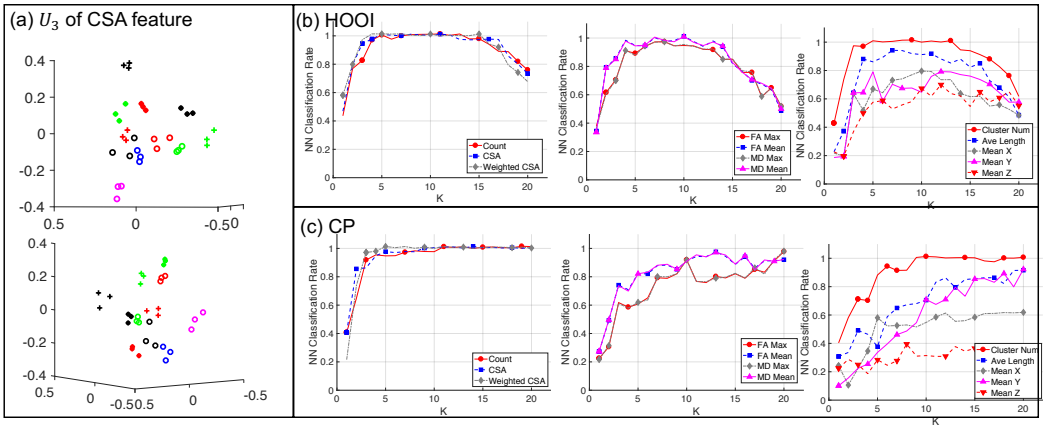

Figure 1: Comparative results on the Sherbrooke Test-Retest data. Part (a) shows the 33 scans, color-coded by subject, in the three-dimensional embedded space for the HOOI and our new CP methods. Parts (b) and (c) show one-nearest neighbor classification results using the low-dimensional embeddings of the HOOI and CP method for various K's and all the connectome features to label the subjects.

increasing values of K. This allows us to simply choose the value of K that explains at least 90% of the variance in the data ($K = 30$ explains over 90% of the variance in all features considered) without worrying about model mis-specification. Also, Figure 1 parts (b) and (c) group the connectome features into end-point features (column one), diffusion features (column two), and geometry features (column three). It is clear that the end-point features are the most robust and discriminative. Overall, these results on real structural connectome data highlight the advantages of our new semi-symmetric CP model for TN-PCA, and specifically the reliability and reproducibility of the resulting low-dimensional embeddings.

: Comparison of Principal Brain Network and the Euclidean Mean

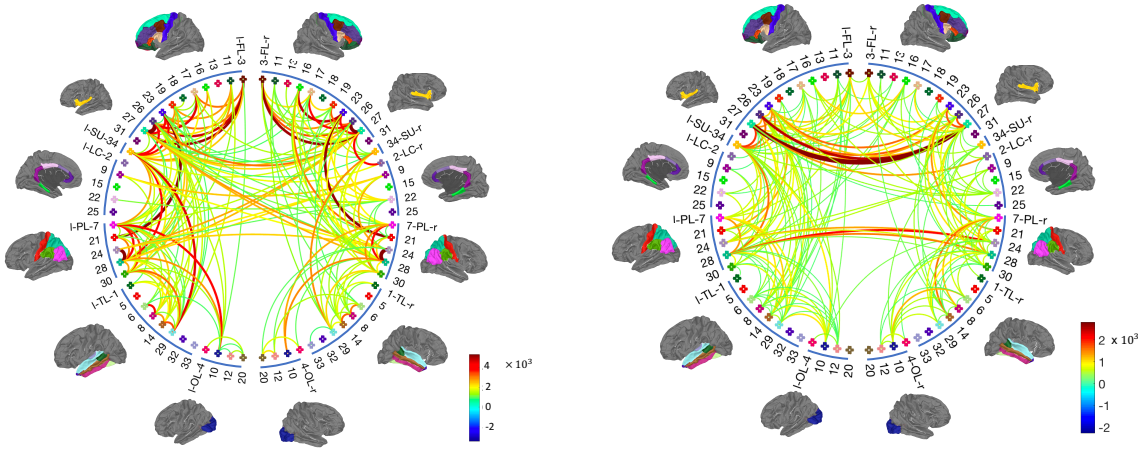

(a) Principal Brain Network (b) Euclidean Mean Network

Figure 2: Comparison of our principal brain network and the Euclidean mean network calculated from the 1065 HCP subjects.

Network: Figure 2 compares our principal brain network with the Euclidean mean network calculated from the 1065 HCP subjects.

Association Between Brain Structural Connectomes and Traits: Figure 3 shows the association between brain structural connectomes and various traits.

Example Subjects in the HCP with High and Low Reading Scores: Figure 4 shows some example subjects in HCP with high and low reading scores.

Example Subjects in the HCP with Light and Heave Alcohol Consumptions: Figure 5 shows some example subjects in HCP with light and binge alcohol consumptions.

Effects of Parcellation and Inclusion of Subcortical Regions: We utilize the data and model generating Table 1 for this study. The difference of correlations between predicted and measured trait scores is used as a met-

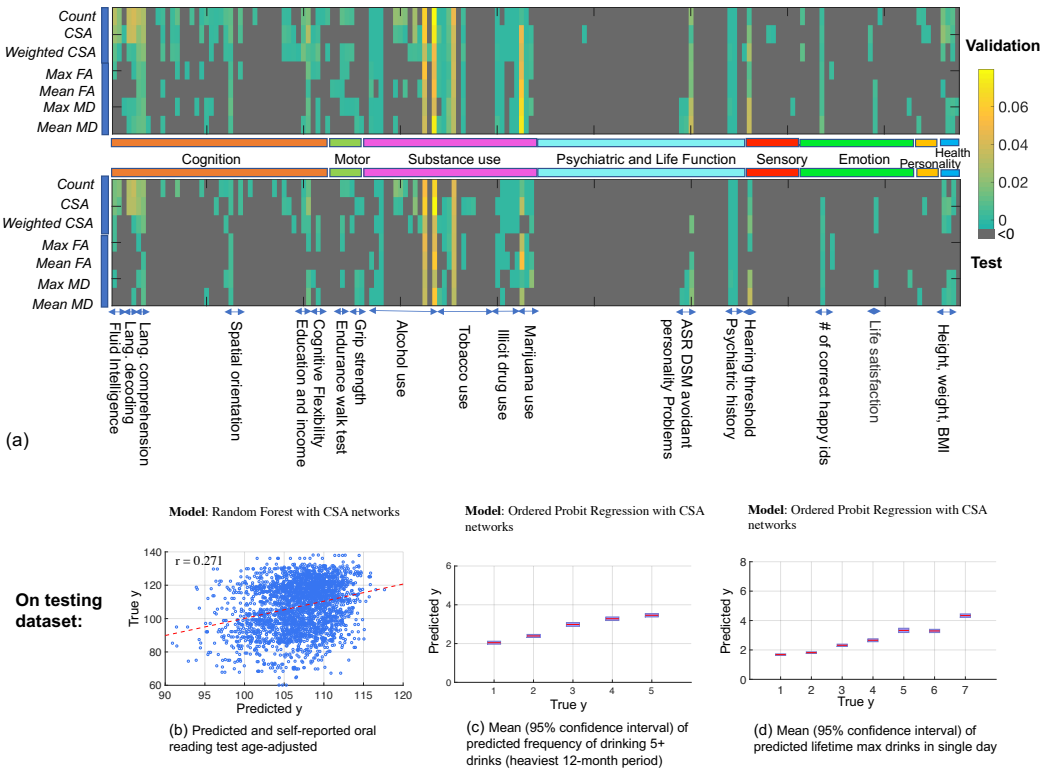

Figure 3: Association between brain structural connectomes and various traits. Panel (a) shows the relative improvement of the predictive power of the full model (with covariates of age, gender and brain network PC scores) over the baseline model (with only age and gender). We threshold the ρ to remove negative ones since in these cases the structural connectome does not help in predicting the traits. Panel (b), (c) and (d) show the predictive performance of the selected machine learning models (based on ρ) on the testing dataset. In these analyses, all 1065 HCP subjects were randomly grouped into a training dataset (75% of subjects) and a testing dataset (25% of subjects). The plots are based on average of 10 runs. In (c) and (d), the red lines and the blue boxes represent the means of predicted Y and their 95% confidence intervals, respectively.

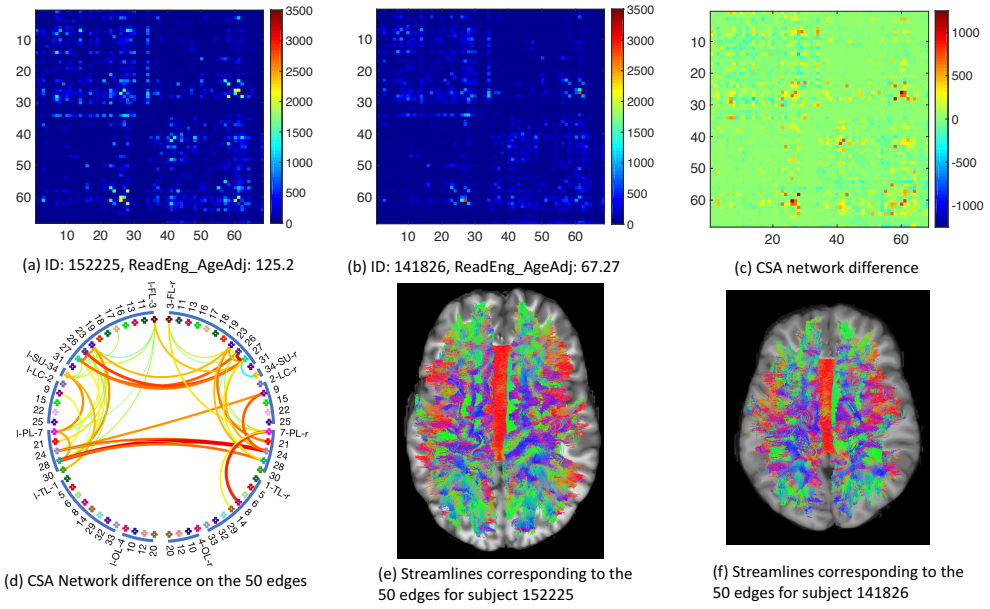

Figure 4: Example subjects in HCP with high and low reading scores. (a) the CSA network for the subject with a high score (HCP ID 152225) and (b) the CSA network for the subject with a low score (HCP ID 141826). (c) shows their CSA network differences ((a) - (b)). (d) shows the network difference on 50 selected edges (according to the Figure 4 in the main paper). (e) and (f) show the streamlines corresponding to the 50 edges.

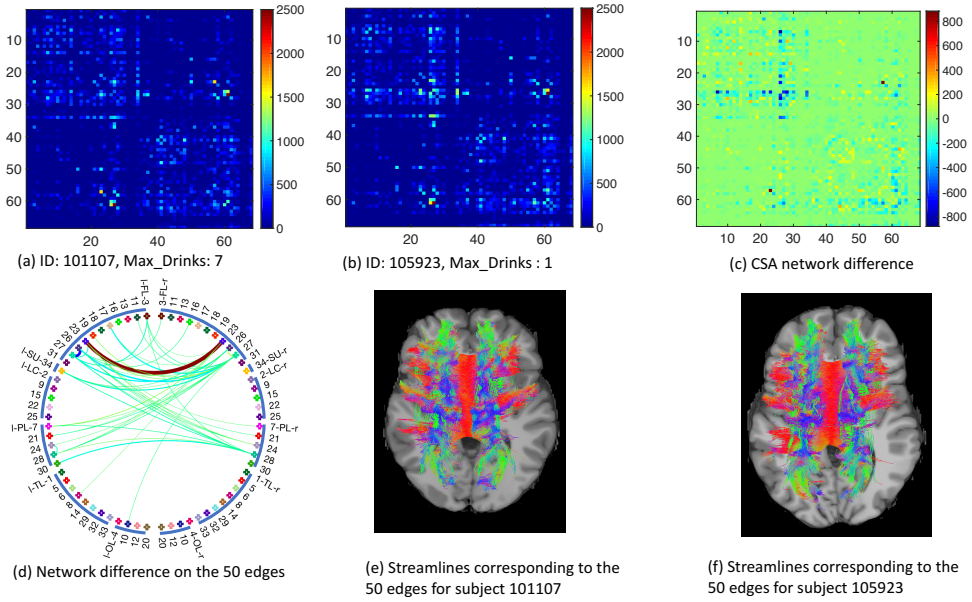

Figure 5: Similar to Figure 4 but for two subjects with light and binge alcohol consumption.

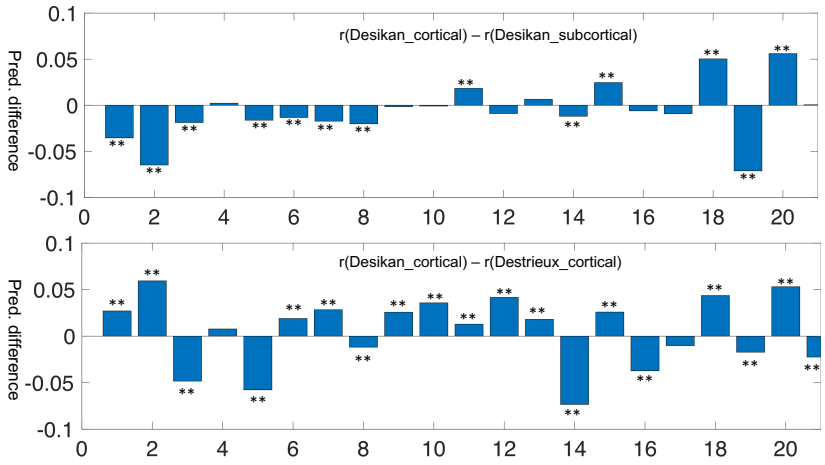

Figure 6: Effects of parcellation and inclusion of subcortical brain regions in prediction of traits. The x-axis is index of traits in Table **??** and the y-axis is the prediction difference. The upper panel compares the prediction difference (difference of correlations between observed and predicted values) without and with subcortical regions using the Desikan parcellation and the lower panel compares the Desikan parcellation (68 ROIs) with the Destrieux parcellation (148 ROIs). ** indicates that the difference is significantly different from zero after FDR control.

ric. In Figure 6, we show two plots: the upper panel compares the prediction difference with and without subcortical regions using the Desikan parcellation and the lower panel compares the Desikan parcellation (68 ROIs) with the Destrieux parcellation (148 ROIs).